

# Multi-Modal, Multi-Energy Approach for Neutron Interrogation of Spent Fuel

## Project #: RSLN-022-19 | Year 3 of 3

Paul P. Guss,<sup>1,a</sup> M. Adan,<sup>a</sup> A. Guckes,<sup>b</sup> E. Bravo,<sup>a</sup> R. Guise<sup>a</sup> B. Gall,<sup>b</sup> J. Tinsley,<sup>c</sup> R. Trainham,<sup>c</sup> A. Barzilov,<sup>d</sup> M. Kazemeini,<sup>d</sup> J. Chagas-Vaz<sup>d</sup> I. Novikov<sup>e</sup> Keith Chase, Gladys Arias-Tapar,<sup>b</sup> Keith Chase,<sup>a</sup> Irene Garza,<sup>b</sup> Adam Wolverton<sup>b</sup> Larry Franks<sup>c</sup>

<sup>1</sup>[gusspp@nv.doe.gov](mailto:gusspp@nv.doe.gov), (702) 295-8095

<sup>a</sup>Remote Sensing Laboratory-Nellis; <sup>b</sup>North Las Vegas; <sup>c</sup>Special Technologies Laboratory

<sup>d</sup>University of Nevada, Las Vegas; <sup>e</sup>Western Kentucky University

The objective of the project is to investigate a non-destructive assay approach capable of quantifying the fissile isotopic composition of spent nuclear fuel and of verifying the declared amounts of special nuclear materials (SNM). This approach takes advantage of the delayed gamma counting of fission product's gamma rays, in combination with the data from the delayed neutron counting. The proposed multimodal neutron interrogation technique combines the measurement of prompt and delayed fission neutrons, induced by a deuterium-deuterium (DD) and/or deuterium-tritium (DT) neutron generator, to differentiate between SNM isotopes while determining quantitative mass values of these isotopes in the item without prior knowledge of the isotopic information. The change in fission rates with differing interrogating neutron energy provides a new technique to independently measure the SNM masses. This study included the simulation of the instrument performance by carrying out modeling of the multi-modal, multi-energy approach for neutron interrogation of samples using Monte Carlo methods. Neutron assay experiments were completed at the A1 source range using a DT neutron generator, two 2"  $\times$  2"  $\text{Cs}_2\text{LiLa}(\text{Br},\text{Cl})_6\text{:Ce}$  (CLLBC) detectors, and various samples.

## Background

Geo-repositories are currently being built for the long-term storage of spent fuel casks. Many of these facilities are scheduled to become fully operational in the early 2020s. Safeguard methods are needed for effectively verifying the contents of spent fuel in casks as they are transferred into the repository and to provide assurance that the stored casks remain intact over time within the repository. Methods to determine U and Pu concentrations in spent fuel when transferred from the storage pool to a storage cask and to verify contents of spent fuel casks as they enter the geo-repository will be required. Our technique involves the assessment of energy

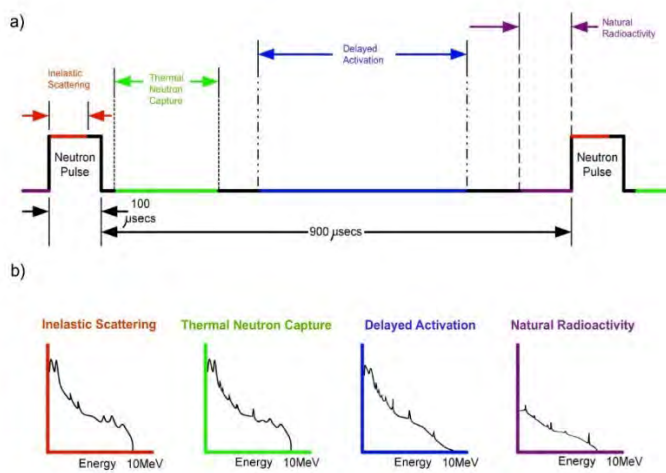


Figure 1. Timing Windows and Sample Spectra. a) Placement of timing windows relative to each neutron pulse. b) Examples of different spectral shapes seen in different timing windows.

distributions of gamma ray and neutron energy spectra as a function of time after the neutron active interrogation irradiation pulse using a commercial neutron generator. See figure 1. ([Bodnarik 2013a](#)).

### ***U and Pu assay methods through radiometric measurements***

Bulk uranium items are often measured using active neutron interrogation systems to take advantage of the high penetrability of neutrons and, therefore, the ability to quickly and effectively measure effective uranium masses in large, dense packaging. These active techniques employ an external neutron source to induce fission in the uranium and subsequently measure emitted fission neutrons. Unfortunately, the fission neutrons from  $^{235}\text{U}$  and  $^{238}\text{U}$  are, for all practical purposes, indistinguishable. Common systems such as the Active Well Coincidence Counter and systems based on differential die-away techniques (which measure prompt induced fission neutrons) or the  $^{252}\text{Cf}$  Shuffler (which measures delayed fission neutrons) require representative calibration standards or known isotopic information to interpret the results, thus limiting the application of these techniques for safeguards purposes (McElroy 2017).

The approach that we employed combines the measurement of prompt and delayed fission neutrons, induced by a DD and/or DT neutron generator (fig. 2), to differentiate between  $^{235}\text{U}$ ,  $^{238}\text{U}$ , and Pu isotopes while determining quantitative mass values of these isotopes in the item without standards or prior knowledge of the isotopic information (Lousteau 2016). The change in fission rates with differing interrogating neutron energy provides the ability of this new technique to independently measure the masses of U and Pu isotopes ([Mozin 2011](#)). Time-correlation measurement could provide information in authenticating the mass and enrichment of SNM objects.



Figure 2. Thermo-Fisher Scientific MP-320 Neutron Generator.

The SDRD project team explored a technique to distinguish between individual fissile isotopes using delayed neutron counting inferred from fitting to the decay curves of the fissile isotopes. Quantification of fissile isotopes using delayed gamma ray counting will be possible once the absolute efficiency calibration of the gamma spectrometer is determined. The new method builds on the existing delayed neutron and delayed gamma ray method ([Venkataraman 2016](#)). Following the delayed neutron counting ([McElroy 2017](#), [McElroy 2016](#)), delayed gamma ray measurements will be performed using our hybrid system of elpasolite detectors ([Mozin 2011](#)).

## Project

The project objective is to investigate a non-destructive assay approach capable of quantifying the fissile isotopic composition of spent nuclear fuel and of verifying the declared amounts of SNM. This approach takes advantage of the delayed gamma counting of fission product's gamma rays, in combination with the data from the delayed neutron counting. The proposed multimodal neutron interrogation technique combines the measurement of prompt and delayed fission neutrons, induced by a DD and/or DT neutron generator, to differentiate between SNM isotopes while determining quantitative mass values of these isotopes in the item without prior knowledge of the isotopic information. The change in fission rates with differing interrogating neutron energy provides a new technique to independently measure the SNM masses.

In the first year of the project, a new data acquisition system was assembled and successfully tested on the bench. To address the challenge of obtaining gamma and neutron energy spectra in different time slices, we prepared a hybrid of the Bridgeport eMorpho electronics to acquire event data that may be tagged by particle identification, energy, and time. Our system is designed to capture these data out to 4 ms following the neutron beam interrogation pulse.

We leverage the concepts proven by [Gozani](#) (2009), [Bodnarik](#) (2013a, 2013b), and [Parsons](#) (2011), and apply these concepts to the nonproliferation field. We acquired a DD and DT [neutron generator produced by Thermo Scientific](#). Leveraging on the SDRD work of [Guss](#) (2015), we can quickly and effectively prepare a dual neutron-gamma ray counter that can establish multiplicity counts of neutrons and gammas for materials interrogated by our neutron sources. What is new in our formulation is the application of the [Bodnarik](#) method of acquiring gamma spectra in fixed time windows to more effectively determine the constituency of the materials, the mass of the materials, and the determination of the presence of SNM and HE.

## Detectors

Following the neutron pulse, delayed gamma ray measurements were performed using our hybrid system and elpasolite detectors (Guss 2013, Mozin 2011). We used non-<sup>3</sup>He neutron detectors that can also measure gamma ray energy with good resolution (elpasolites, for example). See figure 3.



Figure 3. Elpasolite detectors were used to detect both neutrons and gammas.

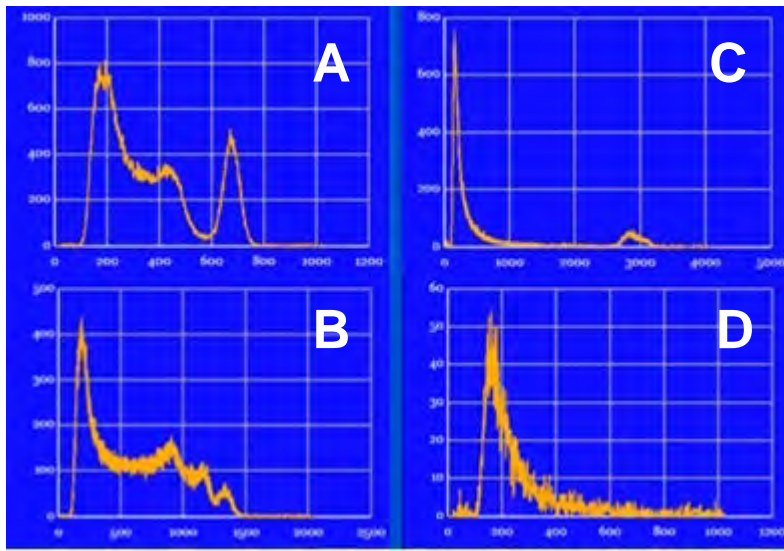


Figure 4. Energy spectra recorded with the elpasolite CLYC detector for A)  $^{241}\text{Am}$  and  $^{137}\text{Cs}$  sources; B)  $^{60}\text{Co}$  source; C)  $^{252}\text{Cf}$  source; and D) Background (no source).

We first collected spectra (fig. 4) for the elpasolite detectors to benchmark their performance. Next, we collected spectra with the Bridgeport eMorpho MCA. Our system acquires list mode data sets. This permitted us to acquire the neutron and gamma data using identical detector geometries, to distinguish between gamma and neutron, to acquire spectra with energy resolution superior to what NaI:Tl can acquire, and to tag the energy spectra in specific time windows following the neutron pulse. Our HvBase from Bridgeport puts out positive HV for an 8-stage PMT and is fully integrated with an MCA.

### Pulse Shape Discrimination

We want to sort events by energy, time, and neutron/gamma discrimination, and the Bridgeport eMorpho event mode appears to have all the necessary ingredients to permit this. Our system used the same detector to detect the prompt and delayed neutron and the gamma.

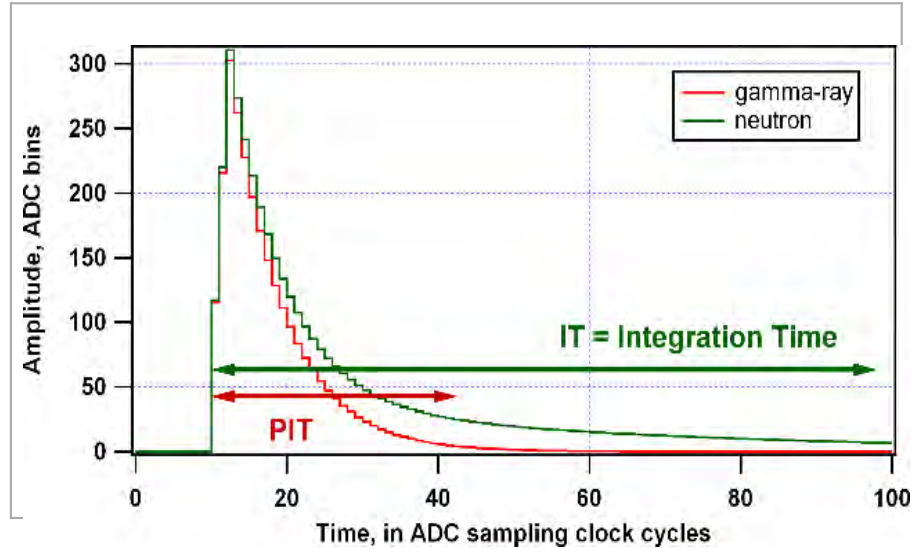


Figure 5. Choosing integration time (IT) and partial integration time (PIT) for the purpose of pulse shape discrimination.

The example in figure 5 shows how to use the IT and PIT parameters for pulse shape discrimination. The graph shows two pulses. The scintillation pulse caused by a gamma-ray

returns to baseline quickly, while the neutron-generated pulse is decidedly longer. We now choose PIT such that it covers the faster pulse and we choose IT to cover the longer pulse.

### ***usbBase Firmware Update***

The Bridgeport eMorpho event mode appears to have all the necessary ingredients to permit sorting events by energy, time, and neutron/gamma pulse shape discrimination. We used two eMorphos with firmware version 4, build 61. We sent two usbBase-8012-P81T to Bridgeport Electronics to update these with the extended list mode firmware version.

### ***eMorpho MCA Acquisition***

The eMorpho units support real-time pulse shape discrimination, which is used in neutron/gamma,  $\alpha/\beta$  – separation and other applications. We investigated adding a real-time scheduler to Linux for the 250-Hz synchronization pulse. For stricter timing purposes, adding the real-time scheduler would reduce added latency that would come to reacting to 4-ms pulses. However, by isolating two of the cores on the embedded CPU, the list mode acquisition and pulse time-stamping can run on individual cores. It is required that the Linux Kernel not interrupt any task running on the isolated core, adding more latency. We are currently using a monotonic clock to determine elapsed time between pulses and start of list acquisition. We established the ability to record timing information between pulses to within a microsecond. Post-processing can be currently done by transferring the data files via thumb-drive. We have done the histogramming for various time windows. The Linux processes outlined in figure 6 are just examples. These can be modified and there is no restriction to use just Linux.

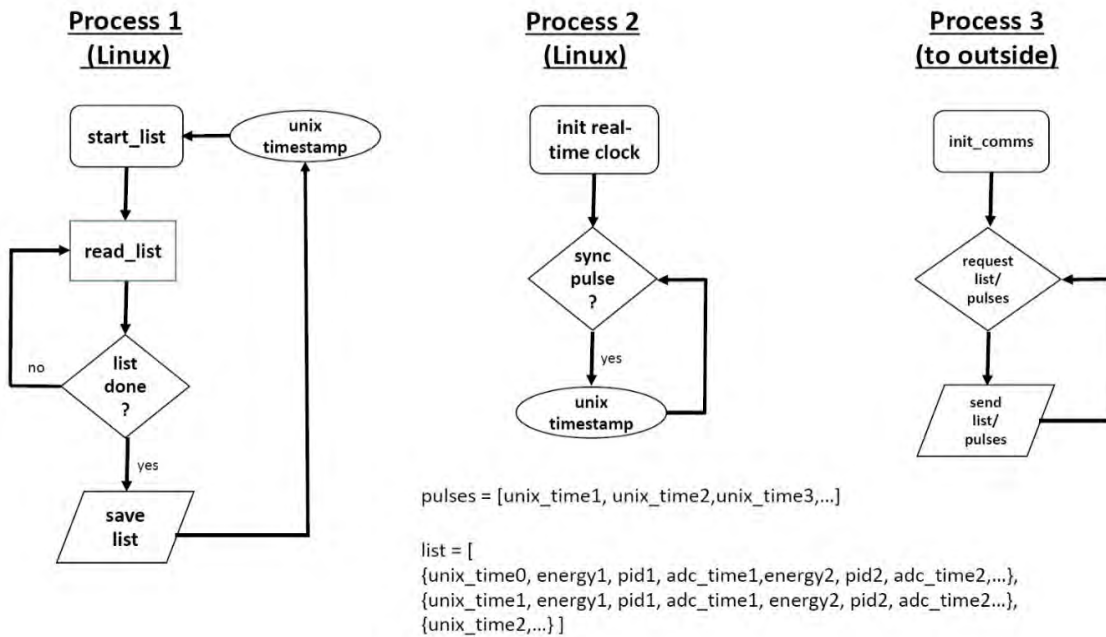


*Figure 6. Examples of Linux processes for buffer read-out.*

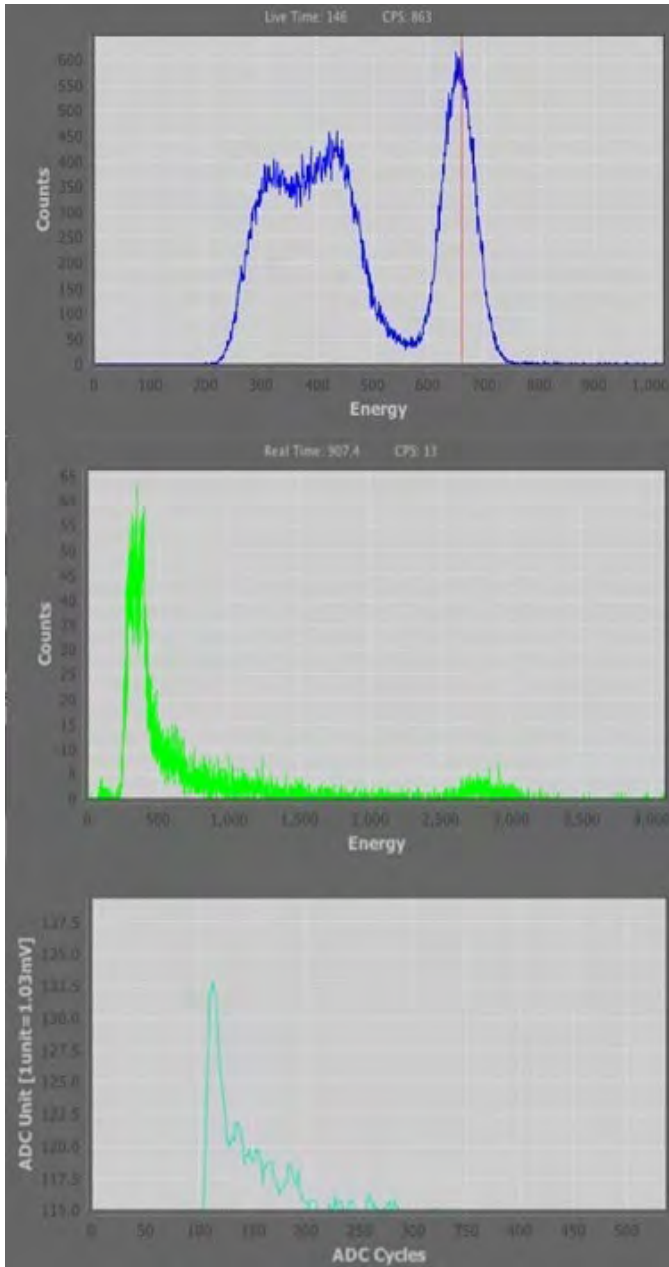


Figure 7. Energy Spectra collected for  $^{137}\text{Cs}$  and  $^{252}\text{Cf}$  radiological and Pulse Trace with  $^{252}\text{Cf}$ .

synchronization pulse with one microsecond resolution using a monotonic clock source. Only two of the tasks produce output. The third task sends the data to the graphical user interface (GUI). This includes log files, i.e. list data buffers and pulse streams. From the list data and time stamps files, the GUI then can display data in a waterfall chart with particle ID. Other capabilities of the GUI include acquiring spectrum, calibrating the detector, and viewing pulse shape traces. In figure 7 are examples of the GUI display for energy spectra for  $^{137}\text{Cs}$ ,  $^{252}\text{Cf}$ , and the pulse shape trace with a  $^{252}\text{Cf}$  source acquired with our buffer read-out system. The project team also began the preparation of the 2-detector time correlation electronics.

The purpose of the Morpho Data Server (MDS) is to provide high-level access to the radiation detectors and their MCAs. It acts as a bridge between the MCAs on the USB side and clients on the internet. Being a true server, the MDS can also be accessed by client software written in 40+ different programming languages. The MDS is a layered software stack. Most often a client gains access through the ZMQ (Protocol layer for robust Transmission Control Protocol/Internet Protocol (TCP/IP) socket communication) server interface – virtually in any programming language they desire. ZMQ (also spelled ØMQ, 0MQ, or ZeroMQ) is a high-performance asynchronous messaging library, aimed at use in distributed or concurrent applications (Hintjens 2013). It provides a message queue, but, unlike message-oriented middleware, a ZMQ system can run without a dedicated message broker. The library's application programming interface (API) is designed to resemble Berkeley sockets (Vessey 1990). Alternatively, client software can access the command layer or the API layer directly using Python. Commands sent to the ZMQ server interface are sent as XML strings. Only the USB-driver depends on hardware and OS. The Morpho Data Server could be run on various machines. There are three tasks that run on the embedded computer. The first task starts at the arrival of an initial synchronization pulse and continuously collects list mode data. The next task timestamps each individual

The embedded computer (fig. 8) is a Raspberry Pi 3 Model B that runs a variant of Linux. Its specifications include a Quad Core with 1.2 GHz Broadcom Chip BCM2837 64bit CPU, 1 GB RAM, BCM43438 wireless LAN and Bluetooth Low Energy (BLE) on board, 100 Base Ethernet, 40-pin extended GPIO (general-purpose input/output), and 4 USB 2.0 ports.

### Targets

For target materials, we considered silicone (<sup>28</sup>Si), aluminum (<sup>27</sup>Al), water (H<sub>2</sub>O), lead (Pb), low enriched uranium (LEU), and depleted uranium (DU). For the first target material, <sup>28</sup>Si, we obtained high purity quartz sand. For the depleted uranium, we accessed three 9-kg plates of DU. After exploiting these materials, we eventually intend to use spent fuel that may be made available at the NNSS for testing purposes.

### API-120 Neutron Generator Campaign

The STL Thermo Fisher Scientific [API-120](#) device is a compact, portable neutron generator for elemental analysis using the associated particle imaging (API) technique, and is housed at the [STL 226 Lab/Shop Goleta Facility](#) that houses the [API-120](#).

The [API-120](#) is portable and compact, less than 15 kg (33 lb.). It uses digital electronics for operational flexibility, and only requires low power, less than 50 watts. The STL [API-120](#) was recently refurbished for another customer project. The unit must run every month or two in order to remove some of the gas pressure due to buildup of <sup>3</sup>He (each year 6% of the <sup>3</sup>H decays to <sup>3</sup>He leading to gas pressure buildup). This was not done previously, and the STL [API-120](#) was sent back to Thermo Fisher Scientific for refurbishment. It now is expected to have ~2000 h of operation life.

The STL [API-120](#) has a yield of ~1.0E+06 n/s. This is two orders of magnitude less than the Thermo Fisher Scientific [MP-320](#). The [API-120](#) indeed appeared to have a strong potential to demonstrate the principals of thesis concept that gamma spectra and neutron spectra for different time windows improve the assay results for active interrogation. However, the [API-120](#) has a yield a hundred times less than the yield of the [MP-320](#). The [API-120](#) then would take one hundred times longer to obtain the same information, i.e. gamma spectra [statistics]. Further, the University of Kentucky had already agreed with UNLV to lease their [MP-320](#) to the project. Until data were acquired, or models adequately performed, it was unknown which unit is optimal for demonstrating the advantage of time-sliced gamma spectra after neutron interrogation. The project team put together the electronics, detectors, and data acquisition system.

The Active Interrogation Experiment at STL with the STL [API-120](#) device was carried out on May 13-17, 2019 STL. The purpose was to gather data using the project-built acquisition system using the STL [API-120](#) device. The objective of this experimental campaign was to demonstrate proof of principle of the concept and viability of getting time vs. energy vs. particle identification active interrogation data, and to learn lessons or technical changes required to participate prior to

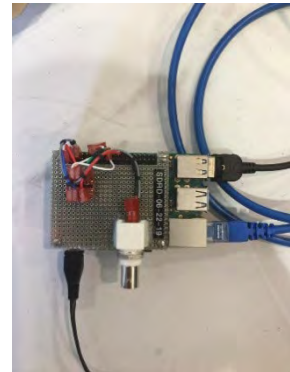


Figure 8. Embedded processor for data acquisition.

the Falcon Dense Plasma Focus Campaign to follow. Benchmarking of the electronics was done while collecting target data, modifications to the GUI were made to support the high-throughput of the data, and some initial post-analysis tools were developed. Figure 9 shows the experimental setup for the target, detector, and neutron generator.



Figure 9. Experimental setup with Aluminum target facing STL API-120 STNG Tube, and CLYC detector.

The goal of the STL experimental campaign was to investigate a non-destructive assay approach capable of quantifying the fissile isotopic composition of spent nuclear fuel and of verifying the declared amounts of SNM. This approach takes advantage of the delayed gamma counting of fission product's gamma rays, in combination with the data from the delayed neutron counting.

The experiments with the STL [API-120](#) device tested the acquisition equipment design and the 2D histogram arrays for MSTS elpasolite detectors, with time on one axis and energy on the other axis. The objective of this experimental campaign was to demonstrate proof of principle of the concept and viability of getting time vs. energy vs. particle identification active interrogation data, and to learn lessons or technical changes required to participate in the Falcon Dense Plasma Focus (DPF) Campaign in June 2019.

The general idea was to irradiate a series of targets and to collect energy spectra in specific time

windows to better improve the signal over the noise of capturing various nuclear interactions and signatures, thereby improving the ability to assay nuclear materials and containers. The energy spectra were collected in the following time windows:

0—2 $\mu$ s	Inelastic Scattering Energy Spectra
2—10 $\mu$ s	Neutron Capture Energy Spectra
10—100 $\mu$ s	Activation Energy Spectra
100—4000 $\mu$ s	“Background” Energy Spectra

The setup is shown in figure 9. We used a pulse to obtain the “start” pulse. After testing the STL [API-120](#) device operation, we established data acquisition with an aluminum target. We next obtained data with aluminum, lead, steel, water, and silicon targets. We generated energy spectra for specific time windows after the “start” pulse.

### ***Dense Plasma Focus Campaign***

The DPF Experimental Campaign I week fell on June 3-7 at RNCTEC; the RSL SDRD team participated. The DPF Experimental Campaign II week fell on June 17-21, 2019. As there were

about 300 or so neutron pulses during the typical experiment day, the more important information we measured was the time distribution of the neutron reaction products. Figure 10 and figure 11 show some of the experimental setup. Figure 12 shows the typical waterfall plot with neutron events in blue and gamma events in red. On close inspection, the pulses of neutrons are evident from this figure.



Figure 11. Setting up the detector table.

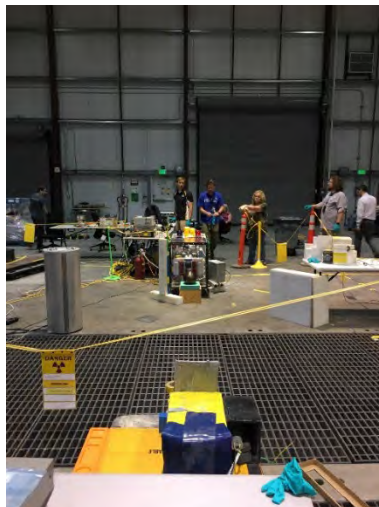


Figure 10. DPF at center. The elpasolite detector setup is to the far right.

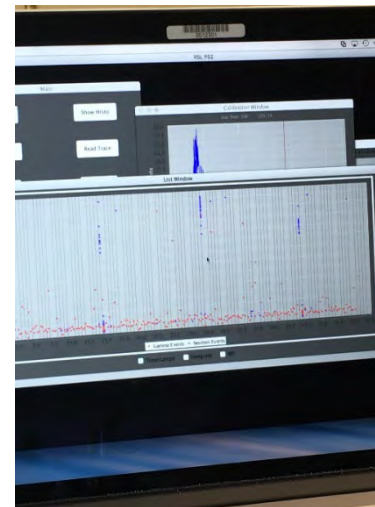


Figure 12. Waterfall display showing energy on the y axis, and time on the x axis. Neutron events are blue, and gamma events are red.

### MP-320 Neutron Generator

In year 2 and 3 of the project, experiments of active interrogation of various samples at the source range - non-fissile materials and DU - using a DT neutron generator (model Thermo MP320) were completed. We performed MP-320 Campaigns in April, October, and June of 2019, October 2020, and June 2021. Western Kentucky University provided the use of their Thermo Fisher Scientific [MP-320](#) Neutron Generator, shown in figure 2. The Thermo Fisher Scientific [MP-320](#) Neutron Generator has a DT Maximum Yield of  $1.0\text{E}+08$  n/s, and a DD Maximum Yield of  $1.0\text{E}+06$  n/s. When fully charged, the [MP-320](#) neutron generator contains  $7.4\text{E}+10$  Bq ( $\sim 2$  Ci  $\pm .05$  Ci) of  $^3\text{H}$  in a sealed system, with wall thickness sufficient to prevent beta emissions. The Thermo Fisher Scientific model [MP-320](#) neutron generator may be employed with either 2.5 MeV neutrons from the DD reaction or 14 MeV neutrons from the DT reaction to present improved isotopic assay. We plan in the future to employ the [MP-320](#) neutron generator with the use of elpasolite neutron detectors that can also measure gamma ray energy with good resolution.

## Modeling

### Computer simulation of instrument performance

Modeling of the multi-modal, multi-energy approach for neutron interrogation of spent fuel was performed using the MCNP6 code (Goorley 2012). The Monte Carlo models of the neutron assay experiments have been run using the following targets: DU, highly enriched uranium (HEU), LEU, Pb, H<sub>2</sub>O, and TNT. The Monte Carlo modeling was also done for plutonium and spent fuel versions.

The assay experiment has been modeled in two models. Model 1 of the neutron assay system consists of the DT neutron source (14.1 MeV neutron energy), the cubic [10 × 10 × 10] cm<sup>3</sup> target, the cylindrical detector cell filled with void, and the shielding/scatterer to protect the detector cell from the “direct” neutron flux from the DT source. The VizEd 3D views and 2D cross-section views of the Model 1 are shown in figure 13. The neutron collision events are also visualized for this model. The materials in the MCNP6 models were set up according to the PNNL’s *Compendium of Material Composition Data for Radiation Transport Modeling* (Williams 2006). The 14.1-MeV isotropic neutron source is set up in a small spherical “cage” cell filled with air. The source is set up in time with 10-microsecond-long square pulse. The delayed emission of neutrons from fissions was set up as discussed in McKinney (2012a). The delayed gamma rays were also calculated.

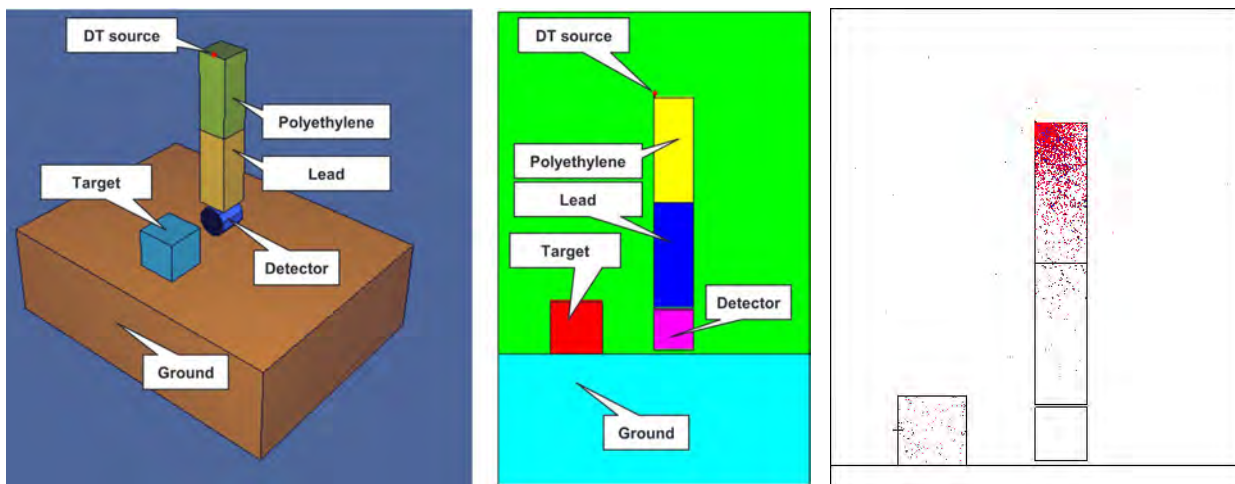


Figure 13. 3D cross-section of Model 1, 2D cross-section of Model 1, and visualized neutron collision events.

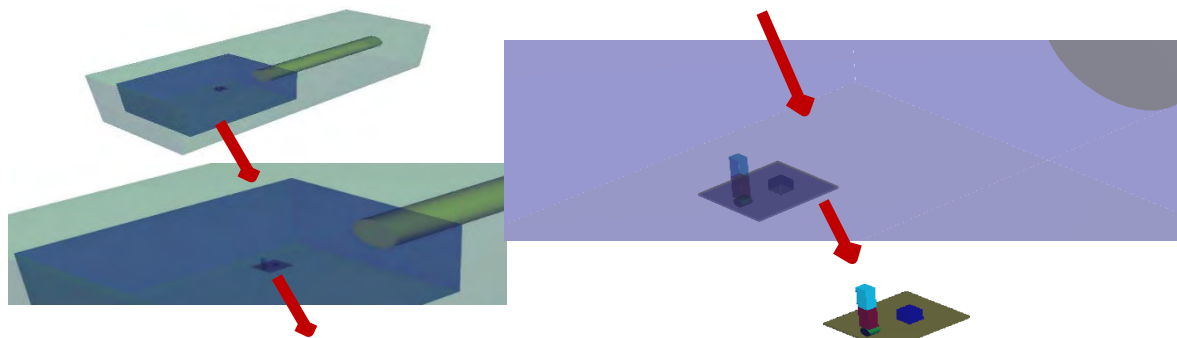


Figure 14. The VizEd 3D views of the Model 2 (the neutron assay system in the source range).

Model 2 includes the neutron assay system as described in Model 1, but the system is placed in the MSTs Building A1 source range where the experiments will be carried out. The VizEd 3D views and 2D cross-section views of Model 1 are shown in figure 14. The MCNP6 input decks for Model 1 and Model 2 were generated. Examples of the tally results for different targets are shown in this report.

Typical results, illustrated for the case of DU are shown in figure 15. Our Monte Carlo calculations in this example addressed the question of how the neutron flux varies in time in the target. The results for neutron fluence (energy spectral distributions) are displayed in the target cell across 200 energy bins from 0.01 MeV to 14.1 MeV in 4 plots for the time windows of 0-10  $\mu$ s, 10-100  $\mu$ s, 100-1000  $\mu$ s, and 1000-10000  $\mu$ s. For each neutron fluence calculation, there is to the immediate right a display of the counterpart photon fluence calculation in the same 200 energy bins from 0.01 MeV to 14.1 MeV also depicted in 4 plots for the time windows of 0-10  $\mu$ s, 10-100  $\mu$ s, 100-1000  $\mu$ s, and 1000-10000  $\mu$ s, for comparison. What is remarkable here is the ability to distinguish different energy spectra of gammas and neutrons in the different time windows. This is further illustrated in the example modeling calculations shown in figure 16. In this case, for a variety of targets modeled, we present a calculation of how neutron flux varies in time in the target for a collection of different targets. This calculation was to study how the neutron flux varies in time in the target using 1000 equal time bins from 0 to 10,000  $\mu$ s (the entire duration of measurements in all time windows). Five energy “groups” were set up (they can be adjusted or new groups can be added): 0 to 0.01 MeV (low energy “moderated” neutrons); 0.01 to 0.1 MeV;

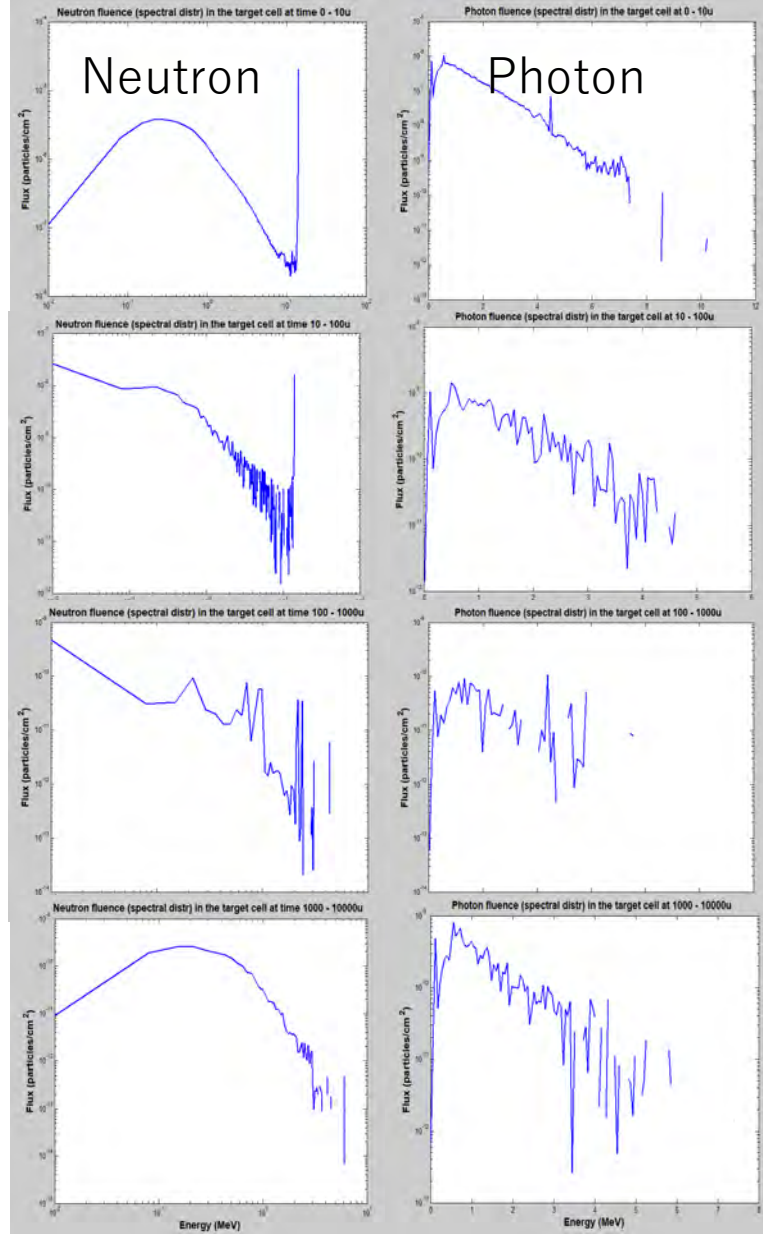


Figure 15. Model 1 Calculation for DU Neutron and Photon Fluence in the target cell for 0-10  $\mu$ s, 10-100  $\mu$ s, 100-1000  $\mu$ s, and 1-10 ms after the neutron pulse.

0.1 to 2 MeV (i.e., the delayed neutrons will be in this energy range); 2 to 13.5 MeV (shown in fig. 16); and 13.5 to 14.2 MeV (DT source neutrons will be in this group). The time scale is in shakes; a square neutron pulse, duration of 0 - 10  $\mu$ s is assumed. These calculations further support the concept of a unique time correlated fingerprint with neutron and photon emission after neutron interrogation.

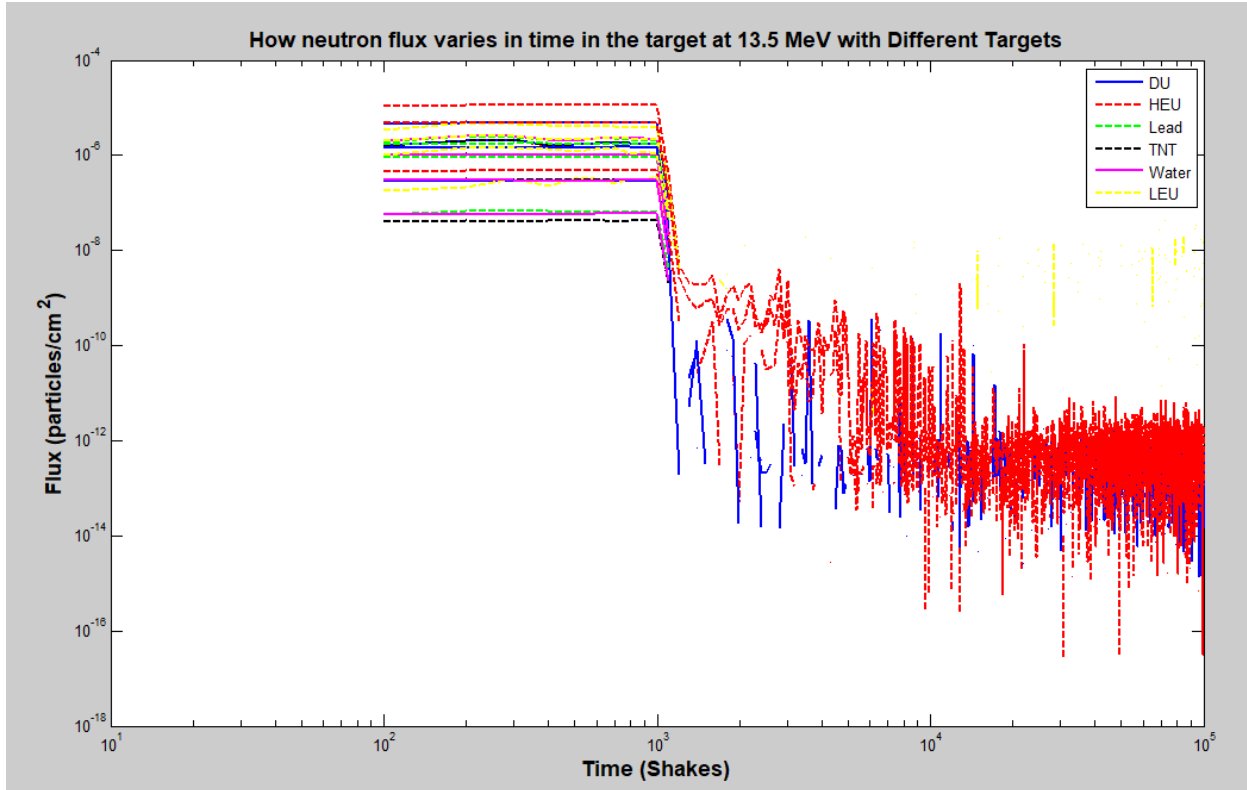


Figure 14. Model 1 calculation of how neutron flux varies in time in the target.

The project team carried out Monte Carlo modeling of multi-modal, multi-energy approach for neutron interrogation of samples using MCNP (Goorley 2012, McKinney 2012a). The modeling of the system was completed for the following configurations of the experimental setup at the MSTS source range: the setup with two CLYC<sub>6</sub> detectors positioned near each other *on one side* of the sample; the setup with two larger-size (the 2"  $\times$  2" cylindrical crystals) CLLBC detectors. The system on the platform in the center of the source range room contains a pulsed DT neutron source, two CLYC<sub>6</sub> or CLLBC detectors protected with the polyethylene and lead bricks from irradiation with fast neutrons emitted by the neutron source, and samples positioned near the detectors.

The input files were prepared per prior methodology. Material cards in the models were coded as prescribed by Williams (2006). The following samples are being simulated: DU plate; aluminum cylinder; water; lead brick; polyethylene brick; and salt. Results of only the calculations for DU are shown in figures below, and these DU results are representative of the full calculation set.

**Two CLLBC detectors, Depleted Uranium Sample: Figures 17-23.**

Cell 33 (detector 1), Tally 4, Gamma Rays, 4 time windows

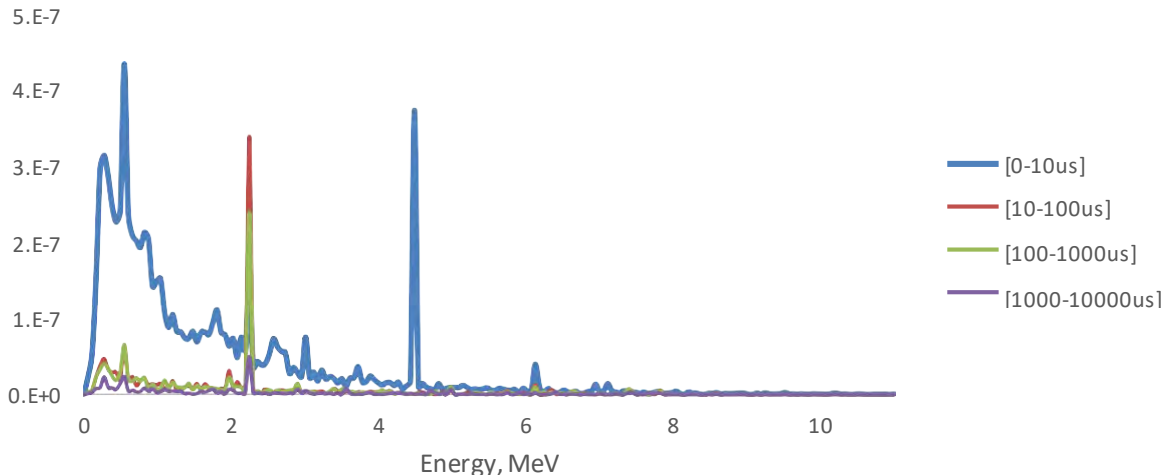


Figure 15. Depleted Uranium, two CLLBC detectors, gamma fluence in the detector 1 (tally F4:P, cell 33); the gamma energy distribution is shown for 4 time windows: [0 to 10  $\mu$ s], [10  $\mu$ s to 100  $\mu$ s], [100  $\mu$ s to 1,000  $\mu$ s], and [1,000  $\mu$ s to 10,000  $\mu$ s].

Cell 33 (detector 1), Tally 14, Neutrons, 4 time

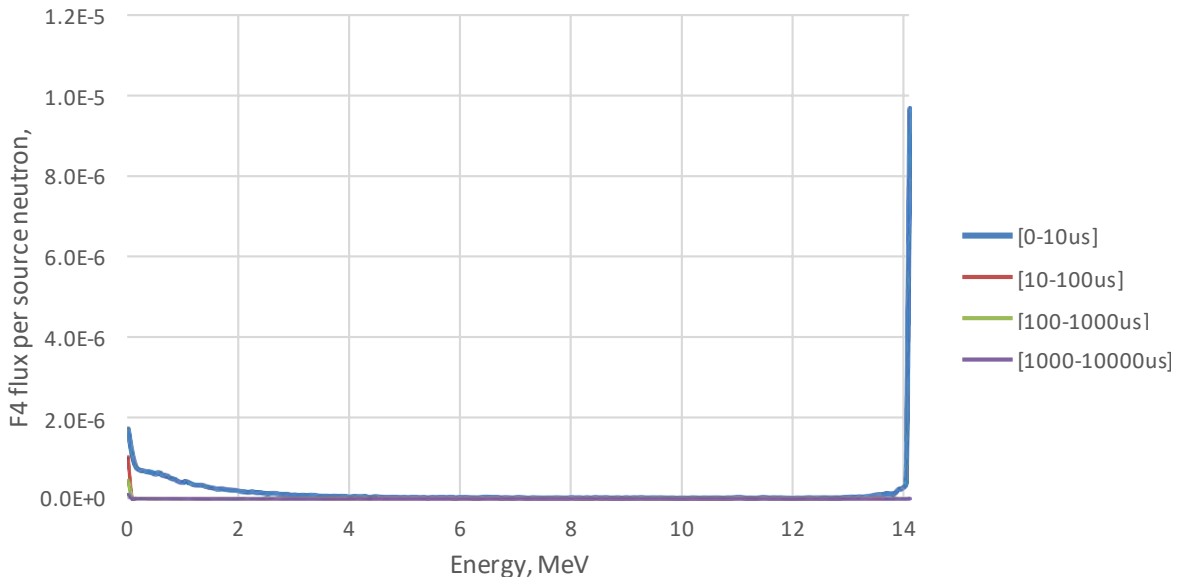
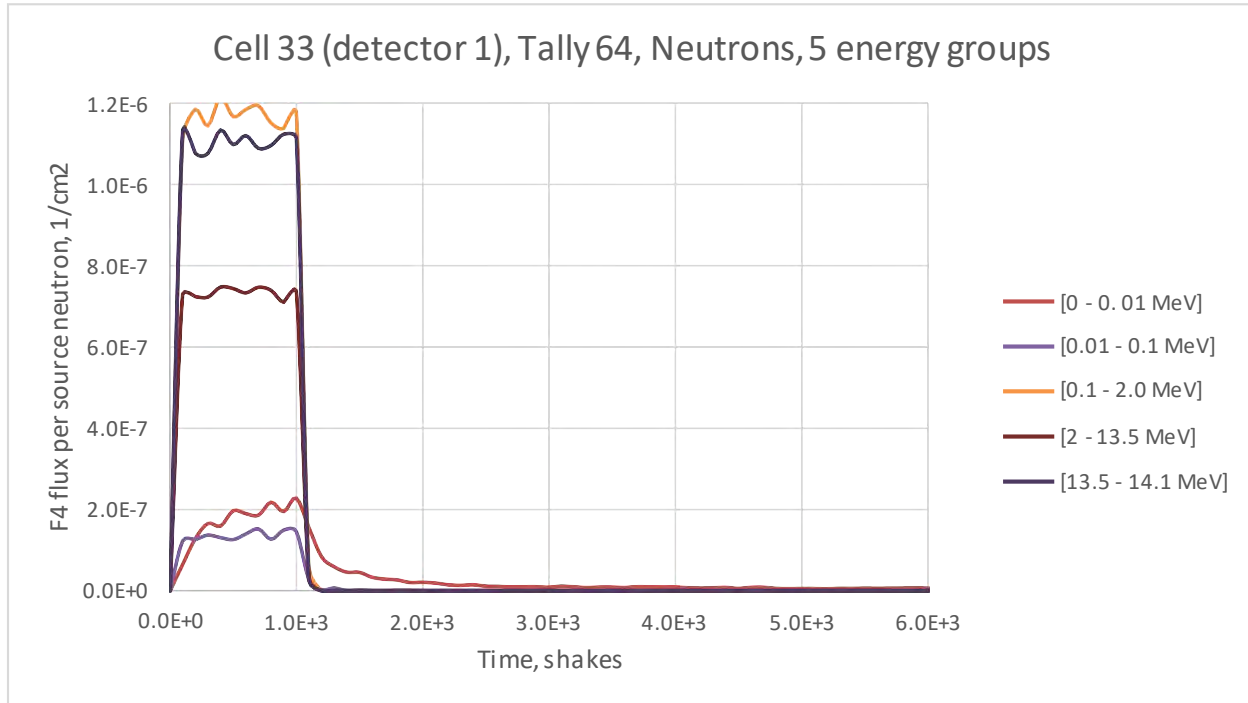


Figure 16. Depleted Uranium, two CLLBC detectors, neutron fluence in the detector 1 (tally F14:N, cell 33); the neutron energy distribution is shown for 4 time windows: [0 to 10  $\mu$ s], [10  $\mu$ s to 100  $\mu$ s], [100  $\mu$ s to 1,000  $\mu$ s], and [1,000  $\mu$ s to 10,000  $\mu$ s].

(a)



(b)

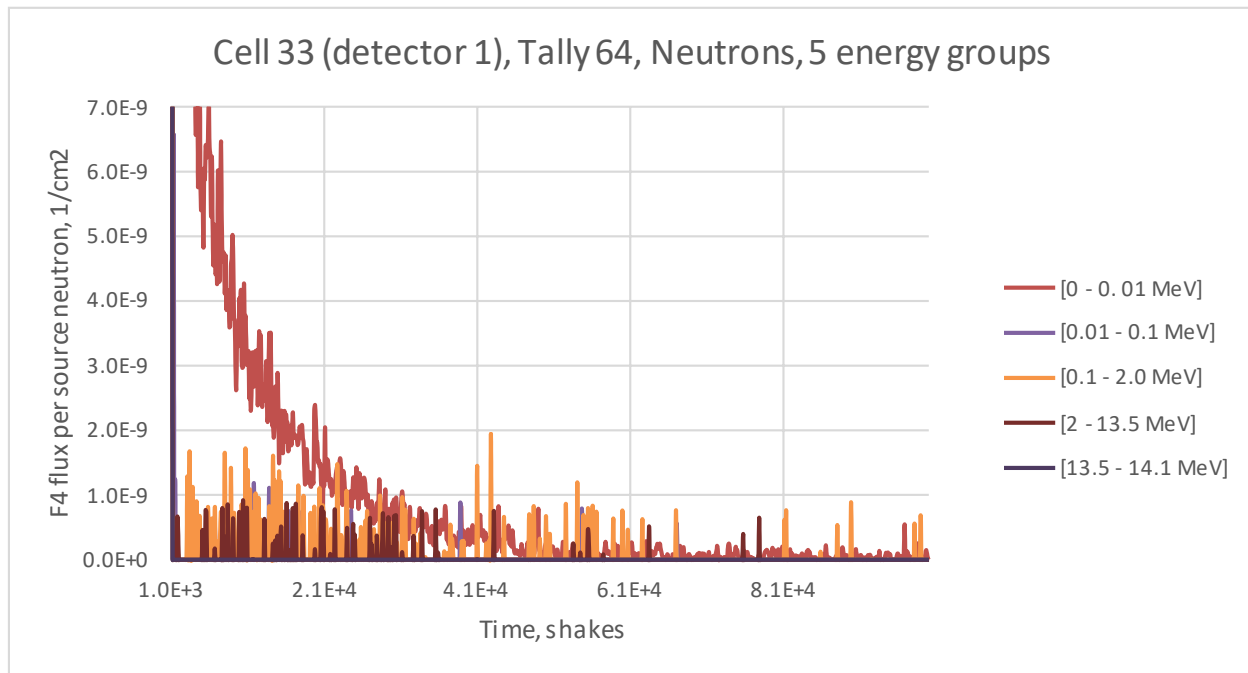


Figure 17. (a, b). Depleted Uranium, two CLLBC detectors, time behavior of neutron flux in the detector 1 (tally F64:N, cell 33); the time distribution is shown for 5 neutron energy groups: [0 to 0.01 MeV], [0.01 MeV to 0.1 MeV], [0.1 MeV to 2 MeV], [2 MeV to 13.5 MeV], and [13.5 MeV to 14.1 MeV]. (a) Time scale is [0 to 6,000 shakes]. (b) Time scale is [1,000 to 10,000 shakes].

### Cell 34 (detector 2), Tally 84, Gamma Rays, 4 time windows

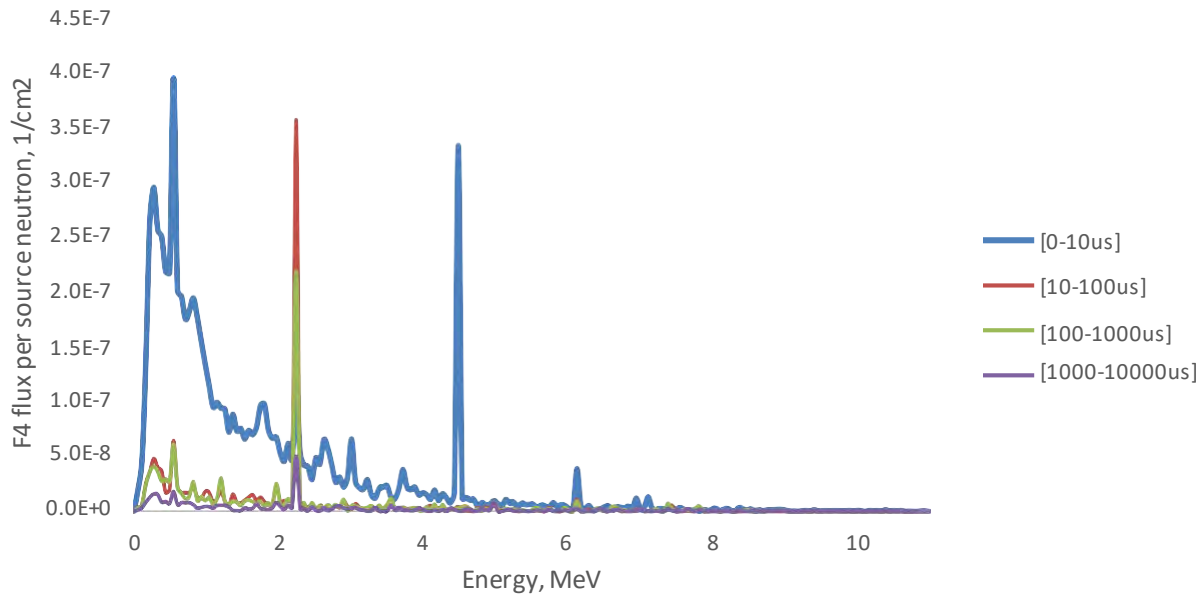


Figure 18. Depleted Uranium, two CLLBC detectors, neutron fluence in the detector 2 (tally F84:P, cell 34), the neutron energy distribution is shown for 4 time windows: [0 to 10  $\mu$ s], [10  $\mu$ s to 100  $\mu$ s], [100  $\mu$ s to 1,000  $\mu$ s], and [1,000  $\mu$ s to 10,000  $\mu$ s].

### Cell 34 (detector 2), Tally 94, Neutrons, 4 time windows

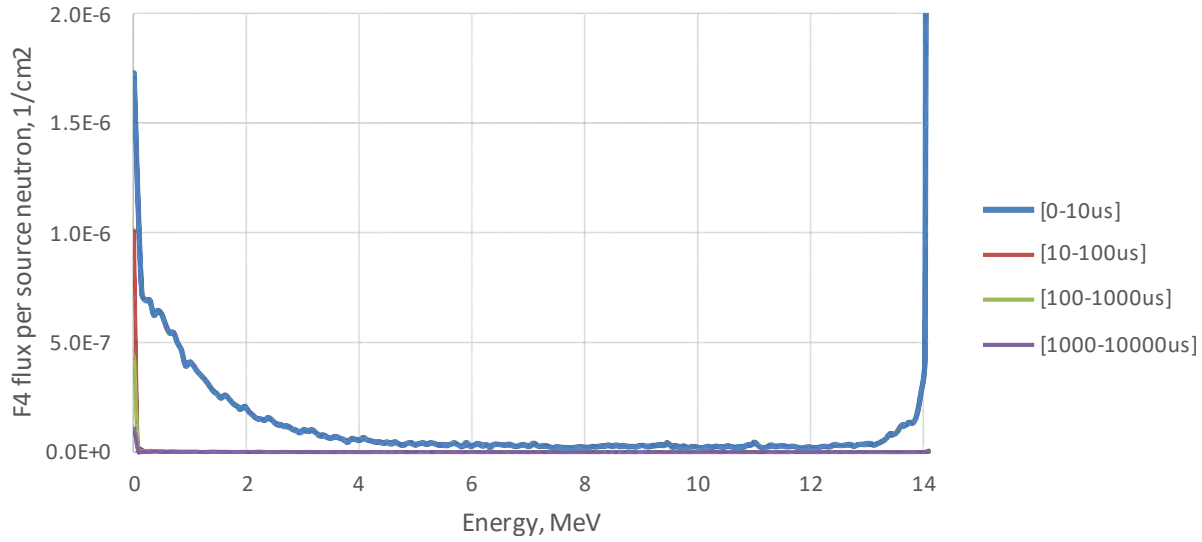
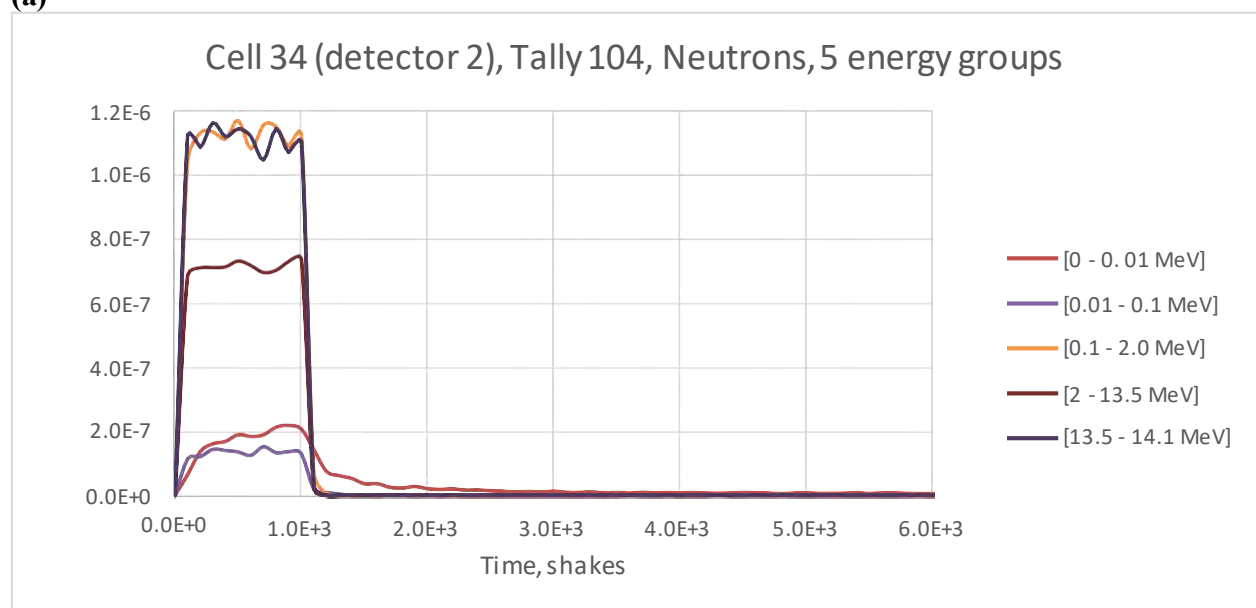


Figure 19. Depleted Uranium, two CLLBC detectors, gamma fluence in the detector 2 (tally F94:N, cell 34), the gamma energy distribution is shown for 4 time windows: [0 to 10  $\mu$ s], [10  $\mu$ s to 100  $\mu$ s], [100  $\mu$ s to 1,000  $\mu$ s], and [1,000  $\mu$ s to 10,000  $\mu$ s].

(a)



(b)

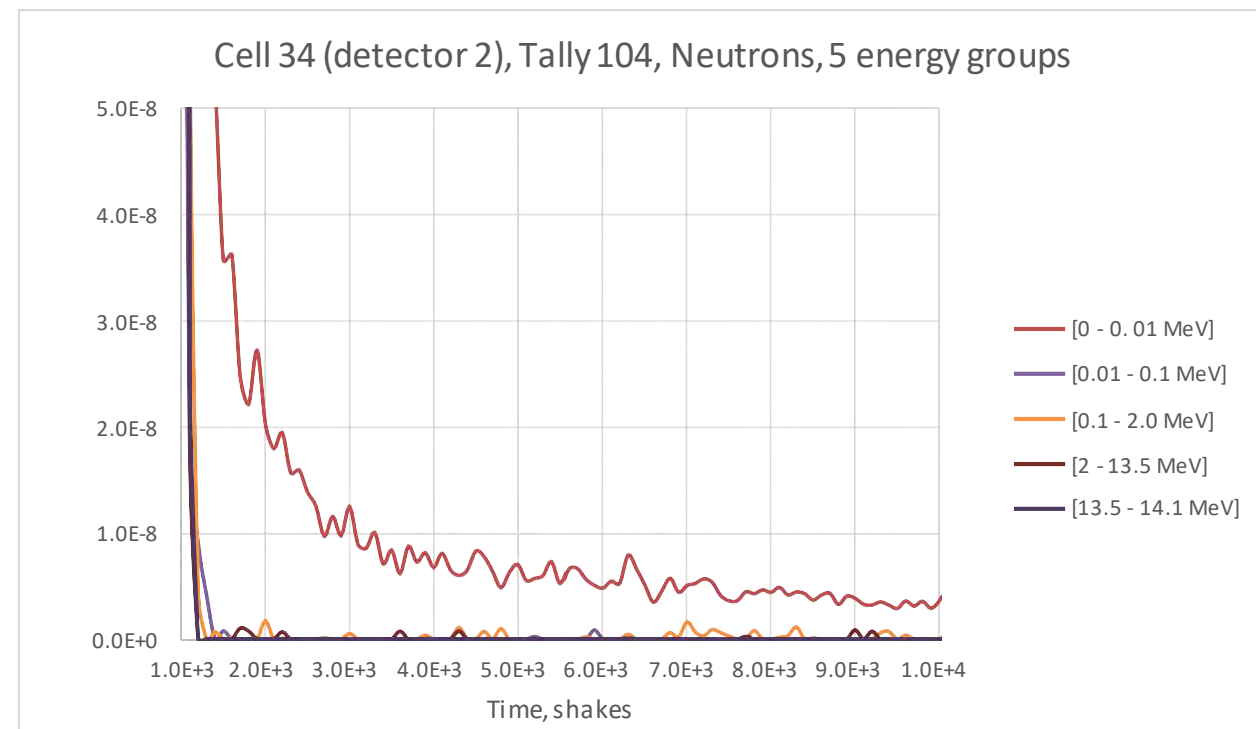
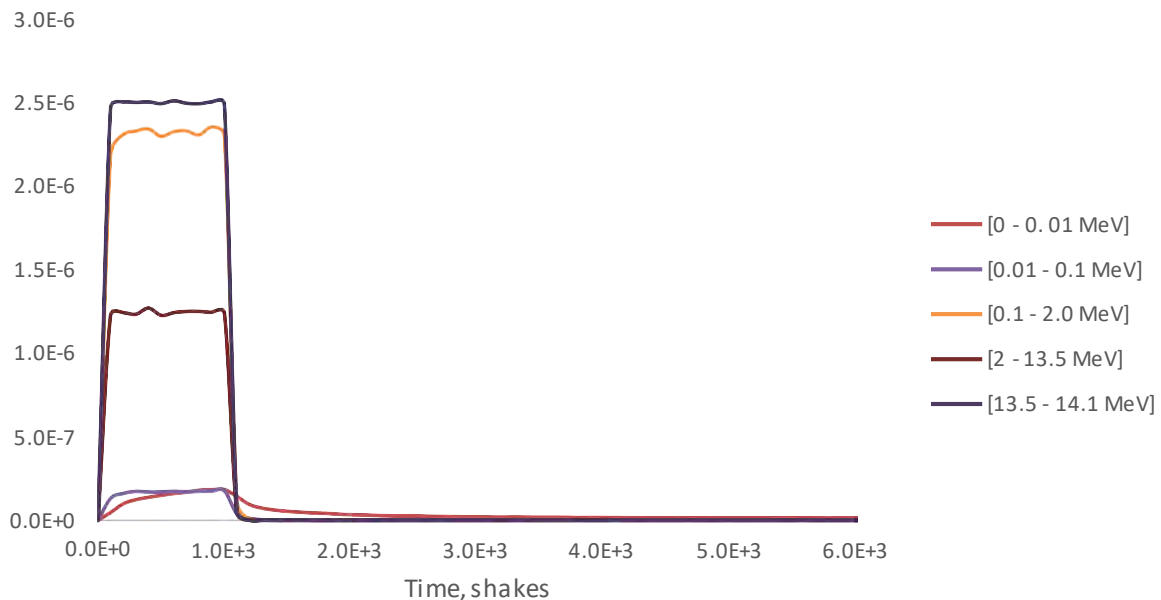


Figure 20. (a, b). Depleted Uranium, two CLLBC detectors, time behavior of neutron flux in the detector 2 (tally F104:N, cell 34) the time distribution is shown for 5 neutron energy groups: [0 to 0.01 MeV], [0.01 MeV to 0.1 MeV], [0.1 MeV to 2 MeV], [2 MeV to 13.5 MeV], and [13.5 MeV to 14.1 MeV]. (a) Time scale is [0 to 6,000 shakes]. (b) Time scale is [1,000 to 10,000 shakes].

**(a)**

Cell 35 (sample), Tally 44, Neutrons, 5 energy groups



**(b)**

Cell 35 (sample), Tally 44, Neutrons, 5 energy groups

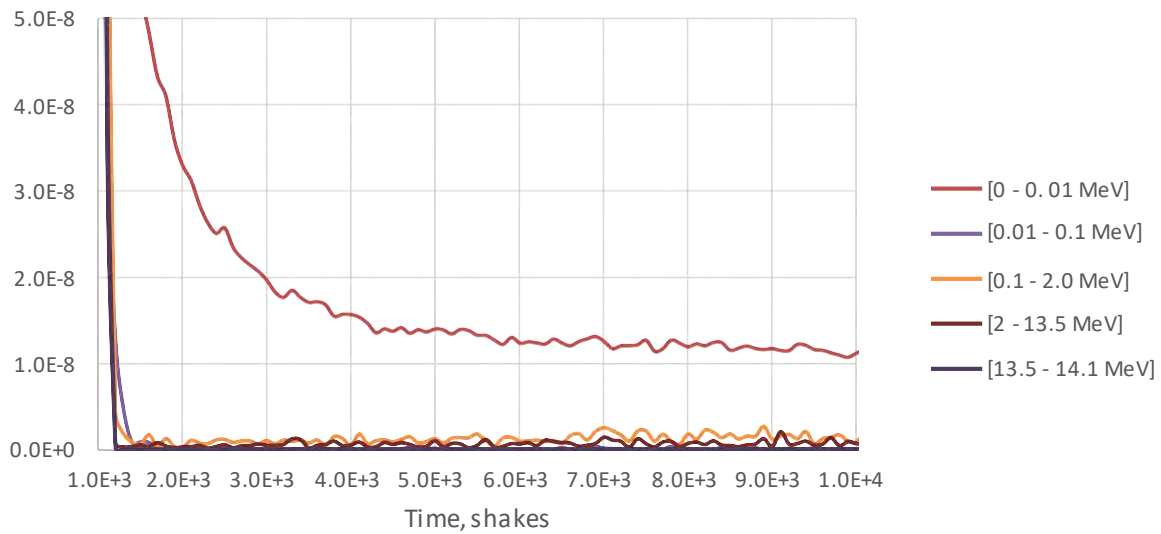


Figure 21. (a, b). Depleted Uranium, two CLLBC detectors, time behavior of neutron flux in the sample (tally F44:N, cell 35) the time distribution is shown for 5 neutron energy groups: [0 to 0.01 MeV], [0.01 MeV to 0.1 MeV], [0.1 MeV to 2 MeV], [2 MeV to 13.5 MeV to 14.1 MeV]. (a) Time scale is [0 to 6,000 shakes]. (b) Time scale is [1,000 to 10,000 shakes].

The energy bins were set at 0 and 20 in order to allow for a quick interpretation of the results (yes or no for the coincident neutron detection). Defining the energy bins in this way allows for quick determination of neutron coincidences as the modeling results show that either a coincidence occurred (non-zero energy bin) or it did not (zero energy bin) (McKinney 2012b). In the case of two detectors (that can be placed either on opposite sides of the sample, or on one side near each other like in the experiments at the source range performed in year 3), only ‘doublets’ might be registered.

Using this approach, the DT neutron assay system with two detectors (CLYC<sub>6</sub> or CLLBC) at the source range was modeled. The model includes the source range environment (concrete walls/floor/ceiling, etc.) and the source-detectors-sample setup on the platform in the center of the room. The setup consists of a pulsed 14-MeV neutron source, two elpasolite detectors protected with the shielding composed of polyethylene and lead to protect detectors from irradiation by fast neutrons emitted by the DT source, and samples positioned near the detectors. Creation of the MCNP input files for the two-detector neutron coincidence model is a significant outcome of this study.

## Spectroscopy

During testing of the electronics using the STL [API-120](#), we collected data for Al, Fe, SiO<sub>2</sub>, Pb, NaCl, H<sub>2</sub>O, and W, as well as background and calibration data. Figure 24 shows typical spectra we obtained during the STL Campaign with the [API-120](#) for Al and W. The electronics appeared to function well, though the count rate was high. The experiment proved the viability of the electronics and the ability to obtain selectable time interval energy spectra. While we hoped to identify different count rates for the reaction, neutron capture, and activation gamma rates, the count rate was so high that we had a high rate of gammas correlated to previous neutron starts which resulted in a loss of synchronization. However, the overall gamma energy spectra are sufficient to distinguish isotopes, given sufficient statistics. The top row in the display presents the classical neutron energy spectrum for an elpasolite detector.

Figure 25 visualizes spectra for the neutron irradiation of DU performed at the NNSS with the DPF. Shown are a gamma 0-4 MeV energy spectrum, a neutron 0-4 MeV energy spectrum, and a combined neutron (blue) and gamma (red) Waterfall 0-4 MeV energy spectrum. We also have similar data for SiO<sub>2</sub>, H<sub>2</sub>O, Al, Pb, and air. Due to the extreme light statistics (<600 neutron starts for all datasets combined), the other data are not shown. However, we learned how to adjust the electronics for low neutron start rates, and we determined how to obtain neutron and gamma time distributions. The data shown also provide a good overview of the display capabilities of the system built by this project.

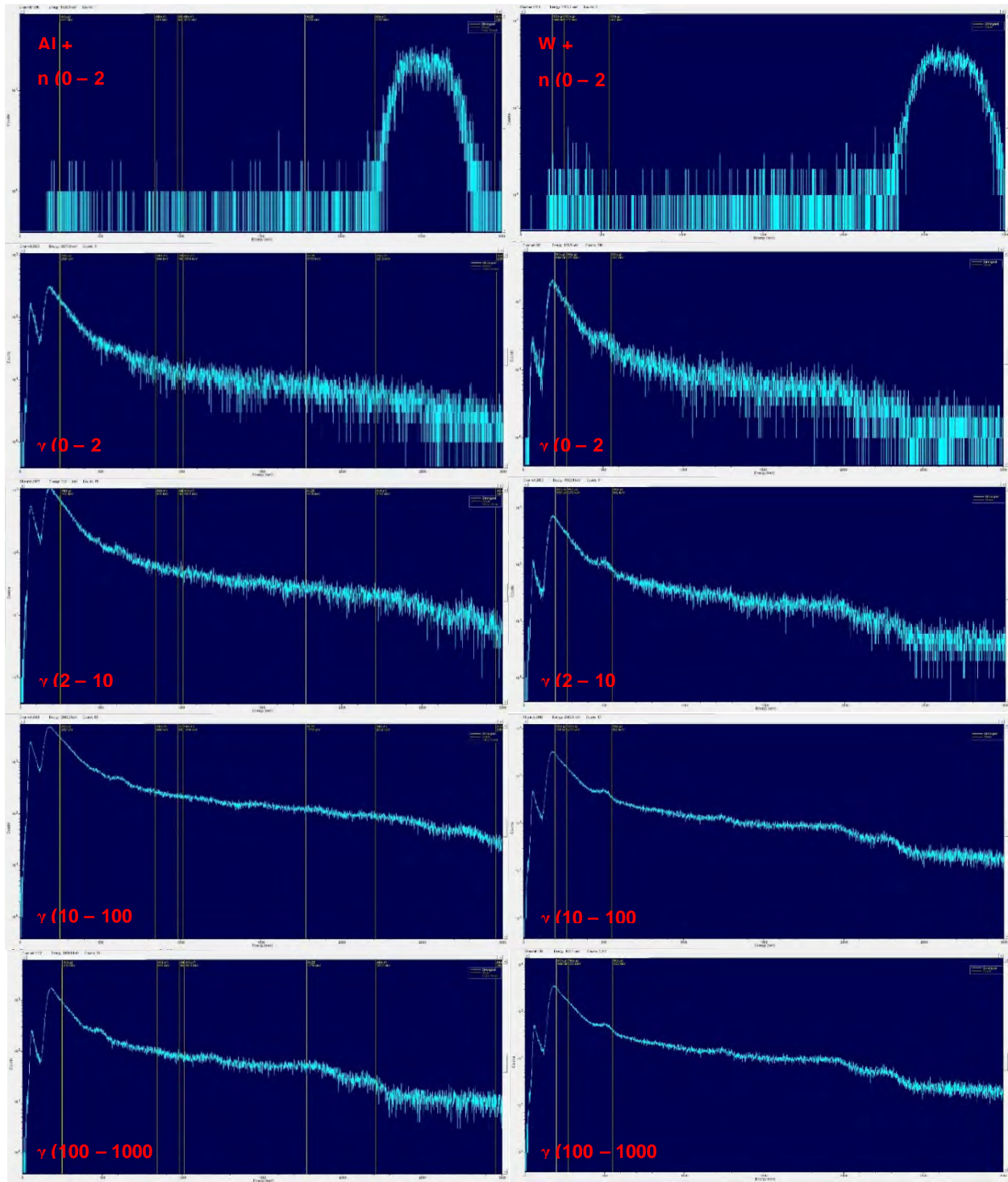


Figure 22. Energy spectra (0 – 3 MeV) for detected neutrons (top row) and gammas in time windows of 0-2  $\mu$ s, 2-10  $\mu$ s, 10-100  $\mu$ s, and 100-1000  $\mu$ s following the neutron start for Aluminum target (left) and Tungsten target (right).

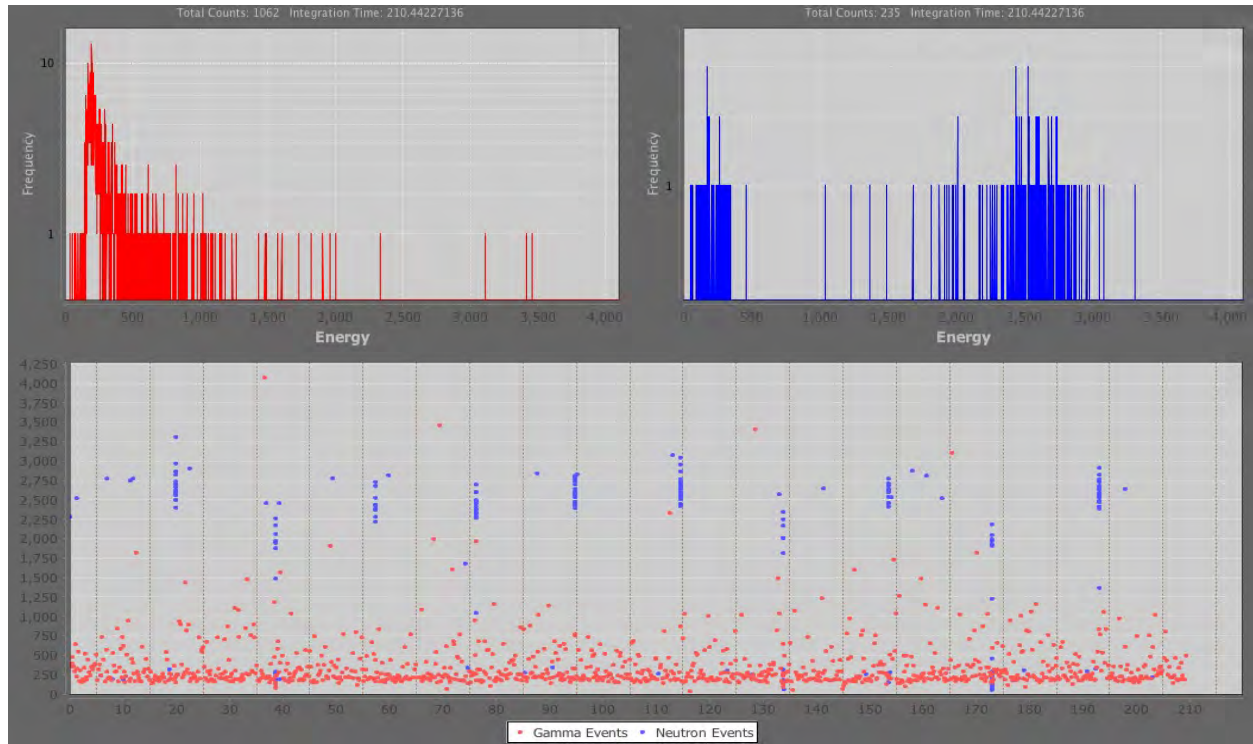


Figure 23. Spectra for the neutron irradiation of DU. Top left: Gamma Energy Spectrum 0-4 MeV. Top right: Neutron Energy Spectrum 0-4 MeV. Bottom: Combined Neutron (blue) and Gamma (red) Waterfall Energy Spectra.

We have demonstrated and have established MCNP modeling methods that test our approach. We have set up 3D histograms by time, energy, and particle ID for elpasolite detectors. The Western Kentucky University MP 320 neutron generator was set up in the A1 Building (see fig. 26). We set up the Bridgeport eMorpho electronics employing a hybrid version of the software. Also, simulations with MCNP were performed for the Pu and the DU response.

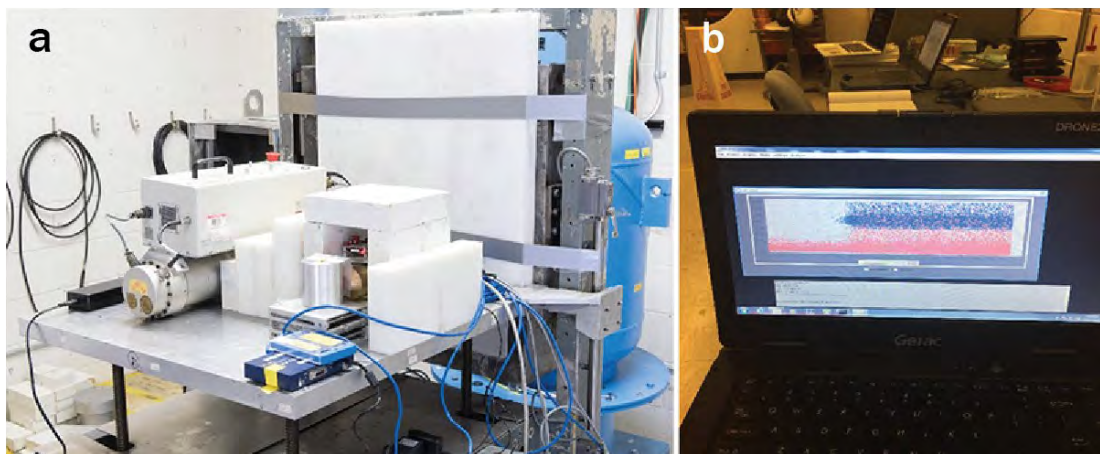


Figure 24. (a) Experimental setup with the MP 320 neutron generator on the left and target on the right. (b) North Las Vegas Building A1 Source Range Control Room in the background; the data acquisition computer in foreground displays an energy spectra waterfall plot of gammas (red) and neutrons (blue).

## Results

The system was deployed on dynamic experiments for the first time, and while results were promising, we must conduct further experiments to confirm the capabilities of the diagnostic. Our preliminary data were consistent with the current literature (Monterial 2015, Dioszegi 2011, Chichester 2009). The [API-120](#) neutron generator had too high a neutron start rate for the electronics we brought; we learned better approaches to set up the acquisition from that campaign. The DPF had too low of a neutron pulse start rate to be useful in reasonable timeframes to collect the spectra we needed. We repeated the physics experiments using the [MP-320](#) neutron generator from Thermo Fisher Scientific Instruments. Additional experiments were conducted in which energy spectra were collected against a 250-Hz neutron start rate. This new diagnostic was used for a variety of experiments where different target materials were used. We expanded the system to include multiple detectors in order to add the event correlation algorithms to further refine the fidelity of the data. The ultimate goal of this project was to map out the parameter space in which our system has the sensitivity and resolution to accurately measure isotopic content of one or more materials.

Two multi-mode radiation  $\text{Cs}_2\text{LiLa}(\text{Br},\text{Cl})_6:\text{Ce}$  (CLLBC) detectors,  $2'' \times 2''$ , equipped with the list-mode digital data acquisition units were used in experiments. These detectors simultaneously recorded neutron and gamma-ray data utilizing a pulse shape discrimination (PSD) technique, adding the time and energy data for each counted detector signal. We measured different gamma energy spectra in the different time windows. We observed that there are different features in different time windows. We do need to subtract out a background component to enhance the differentiation.

This project has contributed to the future mission success of NNSS by developing new capabilities that will contribute to future program development. Being able to distinguish between U and Pu in the same sample has safeguards significance. We have developed the pathway to distinguish between individual fissile isotopes using delayed neutron counting inferred from fitting to the decay curves of the fissile isotopes. Quantification of fissile isotopes using delayed gamma ray counting will result from our technique once the absolute efficiency calibration of the gamma spectrometer is determined. Our new hybrid experimental approach takes advantage of the delayed gamma counting of fission product gamma rays in combination with the delayed neutron counting.

## Conclusion

We have successfully developed and tested a data acquisition system for the neutron irradiation of the spent fuel targets. We have tested in field trials with both an extremely high pulse rate [API-120](#) and a very low pulse rate dense plasma focus neutron generator. We have acquired data with the system to verify its viability for use with a 250-Hz neutron generator. We have completed nuclear modeling work that further supports the viability of our proposed method. In the final year of our work, we demonstrated our system using the 250-Hz neutron generator, and further adapted a 4-detector system that will permit a time-correlation technique to be applied that will increase the fidelity of our nuclear assessment of materials undergoing neutron active interrogation.

We established methods to create time-correlated spectra for the gamma and neutron channels. This new hybrid experimental approach takes advantage of the delayed gamma counting of fission product gamma rays in combination with data from the delayed neutron counting. We can distinguish between fissile isotopes using delayed neutron counting, inferred from fitting to the decay curves of the fissile isotopes. Once we determine the absolute efficiency calibration of the gamma spectrometer, we will be able to quantify fissile isotopes using delayed gamma ray counting results.

With MCNP6 and MCNP-Polimi, we performed modeling and learned statistics are critical. We observed some slight differences in spectra vs. time windows. The project team assessed the MSTS elpasolites detectors. Mark Adan developed the eMorpho electronics. A MSTS procurement loan resulted in the arrival of the WKU MP320. The path forward includes enlarging the detectors, the detector number, and doing a DAF demonstration.

### *Significance*

Being able to distinguish between U and Pu in the same sample has safeguards significance. Energetic neutrons may produce particle emissions in materials with specific isotopic fingerprints. Inferred from fitting to the decay curves of the fissile isotopes, we were able to distinguish between individual fissile isotopes using delayed neutron counting. Quantification of fissile isotopes using delayed gamma ray counting results will be possible once we determine the absolute efficiency calibration of the gamma spectrometer. Our new hybrid experimental approach took advantage of the delayed gamma counting of fission product gamma rays in combination with the delayed neutron counting. This project entailed working with the UNLV Department of Mechanical Engineering. The SDRD project supported a UNLV Graduate Student. It established a tie with Western Kentucky University. It led to a UNLV graduate program paper by Mark Adan entitled “Dual-mode Interrogation System with Irradiation Markers.” The project has direct relevance to and leveraged on the NA-22 DFEAT Program. It also enabled a neutron source for the SDRD Project “Multi-layered avalanche diamond detector.”

### *Tie to Mission/Benefit*

We need safeguards methods for effectively verifying the contents of spent fuel in the casks, both during and after transfer to geo-repositories, and for assuring that the stored casks remain intact over time within the repository. We require methods to determine U and Pu concentrations in spent fuel when transferred from the storage pool to a storage cask and to verify contents of spent fuel casks as they enter the geo-repository and to provide assurance that the stored casks remain intact over time within the repository.

### *Publications, Technology Abstracts*

Adan, M. 2019. “Dual-mode Interrogation System with Irradiation Markers.” UNLV Research Paper for ME 655 – Fundamentals of Nuclear Engineering.

Adan, M. 2020. Remote Sensing Laboratory Pulse Shape Discrimination Application Data Acquisition System Manual, Revision 2. Las Vegas, Nevada: Mission Support and Test Services, LLC.

Gall, B. M. Heika, M. Blasco, J. Bellow, T. Meehan, P. Guss, J. Walker, M. Gerling, Y. Podpaly. 2019. “[Portable Dense Plasma Focus Neutron Source for Mobile Nuclear Non-Proliferation Applications. 2019 Pacific Symposium on Pulsed Power and Applications.](#)” Session 4: Compact Pulsed Power. Koloa, Hawai’i (August 8, 2019). <http://www.p3e.ttu.edu/symp2019/tp2019.pdf>.

Guckes, A. 2020. “Portable Neutron Generator Operations Work Package WP-X120-A01-SDRD-0852.” Las Vegas, Nevada: Mission Support and Test Services, LLC.

Guckes, A., A. Barzilov, P. Guss. 2019. “Directional detection of neutrons and photons using elpasolites: computational study.” *Radat Meas.* **124**: 127-131. <https://doi.org/10.1016/j.radmeas.2019.04.003>.

Guckes, A., Guss, P., Barzilov, A. 2021. “Experimental study of directional detection of neutrons and gamma rays using an elpasolite scintillator array.” *Nucl Instrum Methods Phys Res A*. **992**: 165028. <https://doi.org/10.1016/j.nima.2021.165028>.

Guss, P., M. Adan, A. Guckes, J. Tinsley, B. Gall, A. Barzilov, M. Kazemeini, I. Novikov. 2020. “Multi-Modal, Multi-Energy Approach for Neutron Interrogation of Spent Fuel.” In *FY19 Site-Directed Research and Development*, 14. Las Vegas, Nevada: Mission Support and Test Services, LLC. <https://www.lanl.gov/projects/ldrd-tri-lab/annual-reports.php>.

Guss, P. May 19, 2020. “Multi-Modal, Multi-Energy Approach for Neutron Interrogation of Spent Fuel.” Science & Technology Work-In-Progress Seminar. Las Vegas, Nevada: Mission Support and Test Services, LLC.

Mukhopadhyay, S., R. J. Maurer, P. P. Guss. 2021. “Radiation Detection System Prototypes for Department of Homeland Security.” ANS Annual Meeting Providence, Rhode Island. DOE/NV/03624. (June 13-16, 2021). <https://www.ans.org/meetings/am2021/session/view-582>.

Wagner, E., P. Guss, A. Barzilov, A. Guckes, M. Wolfson. 2016. “Tri-Mode Radiation Detector.” In *FY 2016 Site- Directed Research and Development*, 149-153. Las Vegas, Nevada: National Security Technologies, LLC. <https://www.lanl.gov/projects/ldrd-tri-lab/annual-reports.php>.

#### *TRL Start and End*

Technical Readiness Levels for our concept system started at a TRL ~ 1. We have advanced this to a TRL of at least 2.

## Acknowledgments

We would like to thank Gladys Arias-Tapar, Keith Chase, Irene Garza, Larry Franks, and Rusty Trainham for their contributions to this work.

## References

Bodnarik J., D. M. Burger, A. Burger. G. Evans, A. M. Parsons, J. S. Schweitzer, R. D. Starr, K. G. Stassun. 2013a. "Time-Resolved Neutron/Gamma-Ray Data Acquisition for In Situ Subsurface Geochemistry." *Nucl Instrum Methods Phys Res A*. **707**: 135-142. <http://ntrs.nasa.gov/archive/nasa/casi.ntrs.nasa.gov/20140005993.pdf>.

Bodnarik, J. G. 2013b. "Using In Situ Neutron and Gamma-Ray Spectroscopy to Characterize Asteroids." PhD diss., Vanderbilt University, Nashville, TN. [http://etd.library.vanderbilt.edu/available/etd-04012013-115436/unrestricted/Bodnarik\\_PhD\\_Thesis\\_2013.pdf](http://etd.library.vanderbilt.edu/available/etd-04012013-115436/unrestricted/Bodnarik_PhD_Thesis_2013.pdf).

Bridgeport Instruments. 2019. Data Acquisition Software. 11740 Jollyville Rd. Austin, TX78759, phone: 512-533-9933. <http://www.bridgeportinstruments.com/products/software.html>. Accessed on September 3, 2019.

Chichester, D. L., E.H. Seabury. 2008. "Active Interrogation Using Electronic Neutron Generators for Nuclear Safeguards Applications." INL/CON-08-14196. Idaho National Laboratory. <https://inldigitallibrary.inl.gov/sites/sti/sti/4096530.pdf>. *AIP Conference Proceedings* **1099**, 851. <https://doi.org/10.1063/1.3120173>.

Dioszegi, I., C. Salwen, L. Forman. 2011. "Gamma/neutron analysis for SNM signatures at high-data rates (greater than  $10^7$  cps) for single-pulse active interrogation." *Proc. SPIE* **8018**, 80180D. <https://doi.org/10.1117/12.883912>.

Goorley, T., M. James, T. Booth, F. Brown, J. Bull, L. J. Cox, J. Durkee, J. Elson, M. Fensin, R. A. Forster, J. Hendricks, H. G. Hughes, R. Johns, B. Kiedrowski, R. Martz, S. Mashnik, G. McKinney, D. Pelowitz, R. Prael, J. Sweezy, L. Waters, T. Wilcox, T. Zukaitis. 2012 "Initial MCNP6 Release Overview," *Nucl Technol.* **180** (3): 298-315. <https://doi.org/10.13182/NT11-135>.

Gozani, T. 2009. "Principles and Applications of Neutron Based Inspection Techniques." International Topical Meeting on Nuclear Research Applications and Utilization of Accelerators, Vienna, Austria May 4th-8th, 2009. IAEA. [http://www-pub.iaea.org/MTCD/publications/PDF/P1433\\_CD/datasets/presentations/AP-INT-04.pdf](http://www-pub.iaea.org/MTCD/publications/PDF/P1433_CD/datasets/presentations/AP-INT-04.pdf).

Guss, P., S. Mukhopadhyay. 2013. "Dual Gamma Neutron Directional Elpasolite Detector" STIP DOE/NV/25946— 1813 in Penetrating Radiation Systems and Applications XIV, Gary P. Grim; H. Bradford Barber, Editors, *Proc. SPIE* **8854**: 885402. <https://doi.org/10.1117/12.2021341>.

Guss, P. P., T. G. Stampahar, S. Mukhopadhyay, A. Barzilov; A. Guckes. 2015 “Maximum likelihood source localization using elpasolite crystals as a dual gamma neutron directional detector.” *Proc. SPIE* **9595**: 959502. doi: 10.1117/12.2186179.

<http://spie.org/Publications/Proceedings/Paper/10.1117/12.2186179>.

Hintjens, P. 2013. *ZeroMQ: Messaging for Many Applications*. Sebastol, CA: O'Reilly Media, Inc. <http://shop.oreilly.com/product/0636920026136.do>.

McKinney, G. W. 2012a. “MCNP6 Enhancements of Delayed-Particle Production.” IEEE 2012 Nuclear Science Symposium and Medical Imaging Conference, Anaheim, California, USA, October 29–November 3, 2012, LA-UR-11-06426. Los Alamos National Laboratory.

<https://permalink.lanl.gov/object/tr?what=info:lanl-repo/lareport/LA-UR-11-06426>.

McKinney, G. W. 2012b, “MCNPX 2.7.0 - New Features Demonstrated.” In *MCNPX 2.7.0 - New Features Demonstrated*. LA-UR-12-25775. Los Alamos, New Mexico, Los Alamos National Laboratory.

Lousteau, A. L., R. D. McElroy, J. Hayward. 2016. “A Multi-Modal, Multi-Energy Approach for Neutron Interrogation of Uranium Packages.” In *Proc. 57th Annual Meeting of the Institute of Nuclear Materials Management* (INMM 2016). Atlanta, Georgia, July 24–28, 2016. <http://toc.proceedings.com/32272webtoc.pdf>.

Monterial, M, P. Marleau, S. A. Pozzi. 2016. “Detection and characterization of shielded highly enriched uranium under active interrogation through time correlated fission events.” In *2015 IEEE Nuclear Science Symposium and Medical Imaging Conference* (NSS/MIC), SAND2015-10274C. San Diego, CA, October 31–November 7, 2015. doi:[10.1109/NSSMIC.2015.7581767](https://doi.org/10.1109/NSSMIC.2015.7581767).

McElroy, R. D., S. Croft, D. C. Glasgow, S. Cleveland, J. Knowles, R. Venkataraman, A. Simone. 2016 “Delayed Neutron and Delayed Gamma Counting to Co-detect and Quantify Trace Quantities of Uranium and Plutonium.” In *Proc. 57th Annual Meeting of the Institute of Nuclear Materials Management* (INMM 2016). Atlanta, Georgia, July 24–28, 2016. <http://toc.proceedings.com/32272webtoc.pdf>.

McElroy, R., S. Croft, A. Lousteau, R. Venkataraman. 2017. “Emerging Capabilities for Advanced Nuclear Safeguards Measurement Solutions.” U.S. Department of Energy, National Nuclear Security Administration, NA-22 Office of Defense Nuclear Nonproliferation Research and Development, Novel Technologies, Techniques, and Methods for Safeguards and Arms Control Verification Workshop, Emerging Capabilities for Advanced Nuclear Safeguards Measurement Solutions. Albuquerque, NM, August 29, 2017.

[https://www.inmm.org/INMM/media/Documents/Presenations/Novel%20Technologies%20Workshop/0829\\_0920\\_McElroy.pdf](https://www.inmm.org/INMM/media/Documents/Presenations/Novel%20Technologies%20Workshop/0829_0920_McElroy.pdf).

Mozin, V. 2011. “Improved fast covariance intersection for distributed data fusion.” PhD diss., University of California, Berkeley.

[http://digitalassets.lib.berkeley.edu/etd/ucb/text/Mozin\\_berkeley\\_0028E\\_11805.pdf](http://digitalassets.lib.berkeley.edu/etd/ucb/text/Mozin_berkeley_0028E_11805.pdf).

Parsons, A., J. Bodnarik, D. Burger, L. Evans, S. Floyd, L. Lim, T. McClanahan, M. Namkung, S. Nowicki, J. Schweitzer, R. Starr, J. Trombka. 2011. "Planetary Geochemistry Techniques: Probing In-Situ with Neutron and Gamma Rays (PING) Instrument." 42nd Lunar and Planetary Science Conference, 2011. <http://www.lpi.usra.edu/meetings/lpsc2011/pdf/2379.pdf>.

Venkataraman, R., S. Cleveland, D. Glasgow, J. Knowles, R. McElroy, A. Simone, S. Croft. 2016. "A Hybrid Method Using Delayed Neutron and Delayed Gamma Counting to Co-detect and Quantify Fissile Isotopes" In *Proc. 57th Annual Meeting of the Institute of Nuclear Materials Management* (INMM 2016). Atlanta, Georgia, July 24-28, 2016. <http://toc.proceedings.com/32272webtoc.pdf>.

Vessey, I., G. Skinner. 1990. "Implementing Berkeley Sockets in System V Release 4." In *Proceedings of the Winter 1990 USENIX Conference*, 177-193. Washington, DC, January, 1990. <https://pdfs.semanticscholar.org/92a3/cf739cfe62497f0f2209882550ec8adc2197.pdf>.

Williams III, R. G., C. J. Gesh, R. T. Pagh. 2006. "Compendium of Material Composition Data for Radiation Transport Modeling," PNNL-15870, Pacific Northwest National Laboratory. <https://www.osti.gov/biblio/902408>.